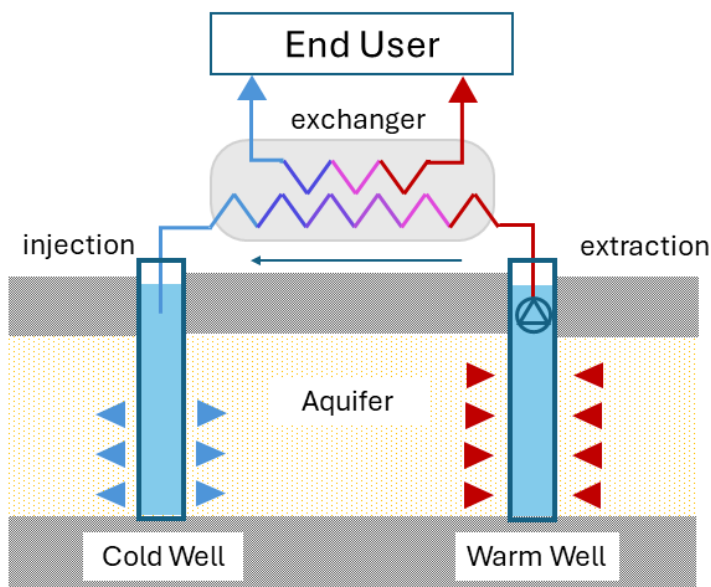


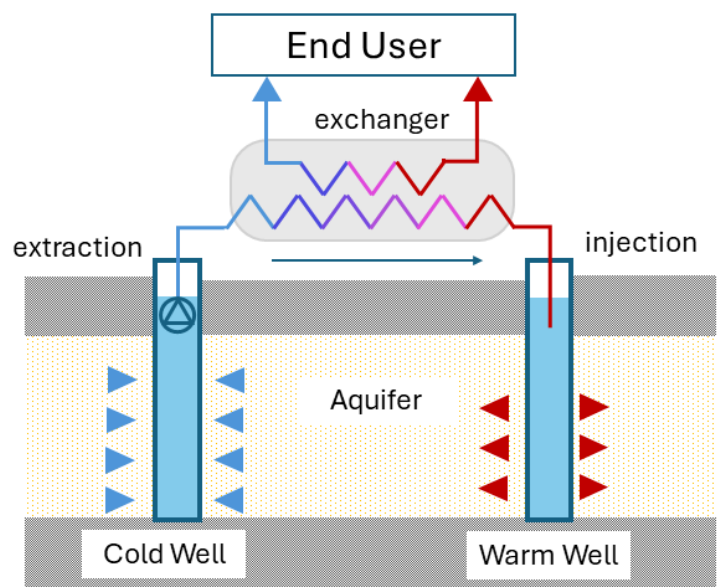
Design Optimization

High Temperature Thermal Energy Storage integrated in District Heating Network

Ziqi Wang



WINTER



SUMMER

Design Optimization

High Temperature Thermal Energy Storage integrated in District Heating Network

by

Ziqi Wang

internship technical report

Student number: 5914620

Project duration: Sep 2, 2024 – Nov 29, 2024

Thesis committee: Kelbij Star,
Jesús Andrés Rodríguez Sarasty,
Ivo Pothof,
Edo Abraham,

Deltares, supervisor

Deltares, supervisor

TU Delft supervisor

TU Delft supervisor

Contents

1	Introduction	1
1.1	Background and motivation	1
1.2	Problem statement	1
1.3	Objectives of the study	2
1.4	Scope and limitations.	2
2	Literature Review	3
2.1	Overview of Thermal Energy Storage Systems	3
2.1.1	Heat storage media based TES	3
2.1.2	Heat storage time based TES	4
2.2	Aquifer Thermal Energy Storage (ATES)	5
2.2.1	Principles of ATES	5
2.2.2	High Temperature Aquifer Thermal Energy Storage (HT-ATES)	5
2.3	Integration of ATES.	7
2.3.1	District Heating and Cooling System	7
2.3.2	System Integration	7
2.4	Optimization for ATES and Challenges	7
3	Theoretical background	9
3.1	Heat transfer between network and the subsurface	9
3.2	Design and operational parameters	11
3.3	Differences with daily storage buffer tanks	12
4	Methodology	15
4.1	Optimization method	15
4.2	Software: rtc-tools	15
4.2.1	library construction	15
4.2.2	Heat Problem	16
4.2.3	Storage component: Buffer	18
5	Buffer Model Setup	19
5.1	Heating Network	19
5.2	Scenarios	20
6	Result Analysis	21
7	Discussion	23
8	Conclusions and recommendations	25
	Bibliography	27

Introduction

1.1. Background and motivation

The processes of urbanization has resulted in a notable increase in energy demand. This is due to a number of factors, including population growth, the development of infrastructure and the growth in transportation. Furthermore, climate change is contributing to an increase in energy demand, particularly for cooling and heating. While fossil fuel and coal-fire are still the leading sectors of the market, its environmental pollution is recognized as a severe problem. In the light of energy transition, seasonal thermal energy storage can be seen as a sustainable alternative. One of the main problem of implementing this kind of sustainable heat energy is that the heat demand and the availability does not match (Figure 1.1). Targeting at bridging the mismatch of seasonal energy demand and supply, Aquifer Thermal Energy Storage (ATES) is recognized as a promising technique to balance the discrepancy by integrating into district heating and cooling network.

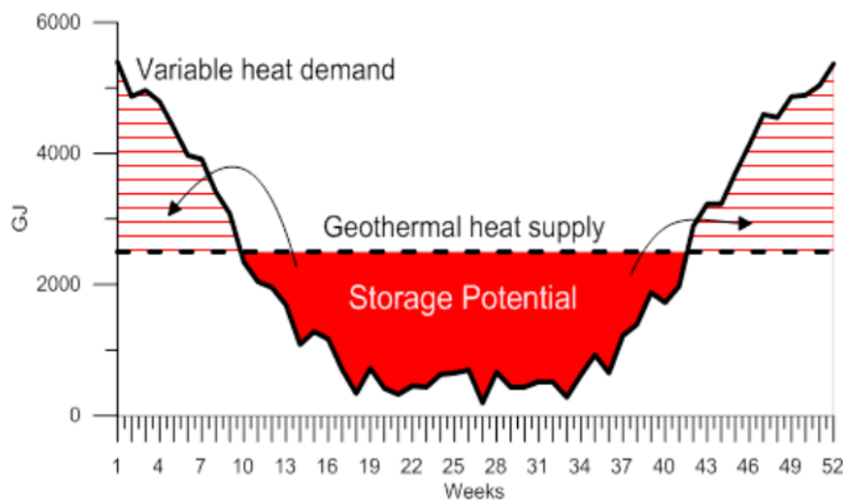


Figure 1.1: Seasonal Mismatch of energy demand and supply, adopted from W.P.Rocchi (2020)

1.2. Problem statement

High temperature Aquifer Thermal Energy Storage (HT-ATES) is distinguished due to its higher storage temperature, yields large potential in system integration. There is a growing interest from the Dutch government and market parties in HT-ATES system with typical storage temperatures between 60 °C to 85 °C. Deltares has contributed to the development of software packages for the stimulation and optimization of heating network such as the Design Toolkit as part of the collaborative research program

WarmingUP. The Design Toolkit contains a HT-ATES component that needs to be improved, tested and validated for the purpose of design optimization.

1.3. Objectives of the study

The objectives of this study are:

1. Review the Thermal Energy Storage (TES) technologies and the related theory of heat transfer. The outcomes of this step are an overview of different storage technologies, a comprehensive understanding into HT-ATES and identification of influential design parameters.
2. Investigate the development of the <https://pypi.org/project/rtc-tools-heat-network/rtc-tools-heat-network>, which is an optimization software developed for energy system. This step is to gain insight into the construction of the storage component in the software, which contributes to the development of the ATES component.
3. Model and optimize the daily storage buffer component integrated in district heating and cooling network. This step is intended to facilitate a deeper understanding of the function and potential of the buffer for optimization, thereby enabling more effective optimization for HT-ATES.
4. Develop an optimization routine for the design optimization of HT-ATES component.

1.4. Scope and limitations

The scope of this study lies in linear optimization of thermal energy storage integration into district heating and cooling system. Daily storage buffer, a feasible technology of thermal energy storage system, is modeled in this project as a TES technology. Linear problem solver is applied in this study for simplification of a complex problem. Thereby, the various underground conditions and heat loss processes are limited considered in this project. The optimization is focus on operational optimization, aiming at compensating for daily peak demand through the activation of the buffer.

The scope is narrowed to daily storage buffer tank and linear optimization due to several constrains. The design of HT-ATES systems is significantly influenced by underground conditions, with numerous design parameters involved. This complexity makes it challenging to accurately model such systems. Design parameters considered in this project including injection temperature and storage volume. Non-linearity is demonstrated between these parameters and the corresponding thermal energy losses in the context of HT-ATES. In order to transform the non-linear relationship into a linear one for the purposes of modeling, the system requires further validation. Consequently, this study is unable to achieve this objective. Furthermore, the optimal storage capacity of an ATES system is heavily dependent on the specific requirements of the district heating and cooling network. Consequently, effective design optimization requires a comprehensive model of the entire district heating and cooling system. The current storage component developed in the software is primarily suited for dialy thermal storage and is constrained by limited storage capacity. These challenges represent the primary limitations of this design study.

2

Literature Review

2.1. Overview of Thermal Energy Storage Systems

In the light of energy transition, energy storage is widely applied as applicable to renewable energy concepts. Energy storage is capable of capturing the residual heat from different heat sources, such as combined heat power plant, solar plants, industrial wasted heat and also for district heating (Zhang et al., 2016). One of the main goal of thermal energy storage is to ensure the balance between demand and supply by allowing the time-wise re-distributions. According to the corresponding storage media, TES can be classified into three main types of systems (Gil et al., 2010): thermo-chemical storage, latent heat storage and sensible heat storage. The maturity of these thermal storage technologies can be assessed with technology readiness level (TRL). The corresponding TRLs are increasing in the above mentioned order, indicating that the sensible heat storage is the most ready for market (Guelpa & Verda, 2019). A summary of the classification of various types of thermal energy storage technologies are presented as Figure 2.1.

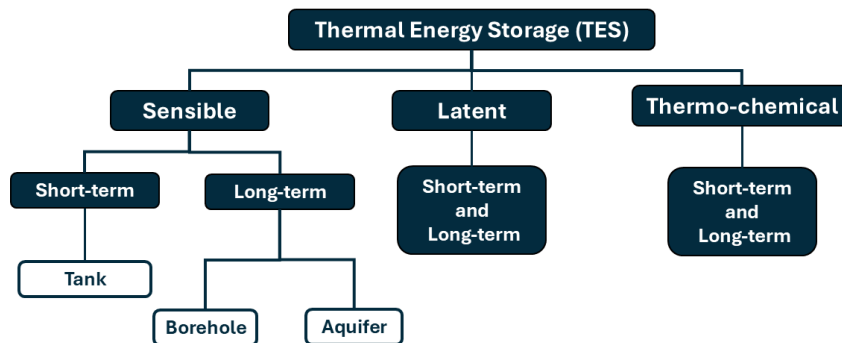


Figure 2.1: Classification of thermal energy storage technologies, adopted from Guelpa and Verda (2019)

2.1.1. Heat storage media based TES

The subsequent sections will present an overview of the aforementioned types of heat storage technologies. The storage media and the theory are briefly introduced, followed by an analysis of the strengths and drawbacks.

Thermo-chemical energy storage

Thermo-chemical energy storage makes use for heat energy from reversible chemical reactions. The endothermic process energy (heat), which can be stored as long as desired until the reverse (exothermic) process, is forced. The released energy resulting from the exothermic process can be used immediately for domestic hot water and heating building applications. Since the storage takes place when formulating molecular bonds, the energy can be fully captured if the generated material is kept at certain conditions (Solé et al., 2015). Hence, this type of chemical energy storage enables to bridge long duration periods between supply and demand (seasonal difference) without the limitation of heat losses in time (Sadeghi et al., 2024). While this type of technology shows a promising future, the corrosion of metals used to build up reactors is one of the main drawbacks to overcome (Alva et al., 2018).

Latent heat storage

Latent heat TES (LH-TES) systems store energy in the latent heat of the materials during a constant temperature process like phase change (Alva et al., 2018). Phase change materials with solid-liquid transition are considered to be more efficient comparing to materials of other type of transition (Guelpa & Verda, 2019). While liquid-gas phase change has the highest latent heat, the enormous change in volume of the materials is the main constraints of its application. Comparing to sensible heat storage, LH-TES systems are capable of storing thermal energy in a smaller volume and reducing in the storage media cost. However, more challenges are encountered when implementing this type of systems. The heat transfer design is more complicated comparing to sensible heat storage, which requires an elaborated design. The choice of heat transfer medium is a crucial aspect of system design. For instance, the current experience with low temperature salts has shown a notable decline in performance after a moderate number of phase change cycles, as evidenced by reference (Gil et al., 2010). This highlights the importance of careful consideration when selecting the appropriate medium.

Sensible heat storage

Sensible heat TES (SH-TES) is the most widely used type of daily storage combined with District Heating (DH). In SH-TES, the temperature increase (or decrease) of the storage medium is used to store heat (or cold). Materials used for sensible heat storage undergo no phase change during storage application. The selection of material is done based on physical properties (such as the specific heat capacity, density, and thermal conductivity), availability and price (Guelpa & Verda, 2019). Water is one of the most commonly used fluid material due to its circularity and accessibility. It can be suitable for energy storage below 100 °C and is used for heat transport in distribution pipelines.

2.1.2. Heat storage time based TES

This section presents the application of TES for both short-term and long-term usage, with a particular focus on the implementation of various forms of sensible heat storage. The detailed analysis of short and long-term usage for latent and thermo-chemical heat storage is included in the research of Guelpa and Verda (2019).

Short-term storage

Short-term storage system intends to overcome the gaps between demand and supply on hourly and daily bases. This type of system is developed to ensure a stable heat supply during the day and increase the energy efficiency. It is usually possible to preserve heat in these systems at a temperature that is appropriate for the end user, given the relatively shorter storage time and lower heat loss (Pompei et al., 2023). Water tank storage system, also known as buffer, are designed mainly for short term storage. Tanks for thermal storage consist of a concrete or steel container filled with storage volume. This type of application can be constructed above or below ground.

Long-term storage

Long-term storage is designed to store heat for a longer period of time (weekly storage to seasonal storage) and release it when demand is high. In the context of seasonal storage, the application of long term storage aims to redistribute thermal energy in different seasons, thus stabilizing the supply from the source, without using additional sources when demand peaks in certain seasons of the year. In this way, the heat from the source during largely available seasons can be of better usage, increasing the annual energy efficiency. As a result of the increased storage period, the heat loss of the system is

larger comparing to short-term storage. A typically heat loss of long-term storage is 30% of its injected thermal energy, while the short-term storage losses less than 5% (Guelpa & Verda, 2019). Therefore, long-term storage requires the systems to have a larger storage capacity comparing to short-term storage, and an acceptable heat loss during the storage period.

One of the widely implemented technologies is borehole (or duct) thermal energy storage (BTES), which exploits the heat capacity of the soil to store heat. The main component of the system is the borehole heat exchanger (BHE) containing U-tubes filled with heat transfer fluid, and the grout material filling the space between the U-tubes and the surrounding ground. It is suitable for large scale seasonal storage because of an easily increased storage volume (Lanahan & Tabares-Velasco, 2017), by increasing the number of BHE through drilling. Additionally BTES does not require specific geographical formation as with Aquifer thermal energy storage (introduced in 2.2) systems, therefore more universally applicable (Lanahan & Tabares-Velasco, 2017).

2.2. Aquifer Thermal Energy Storage (ATES)

Aquifer thermal energy storage (ATES) is most designed for seasonal storage. It is developed to store thermal energy within an aquifer, utilizing the heat capacity of water. Aquifers are geological systems of water-bearing materials with a certain porosity, which allows the existence of groundwater. Two confined layers, consist of rock or clay, present at the top and bottom. This allows the aquifer to behave like a container. Groundwater retained in the aquifers can be extracted and re-injected through penetrating wells after cooled down or heated up period. Thermal energy is stored in the aquifer, whereas groundwater is used as heat transfer medium. The systems are general designed to work during the lifetime of 30 to 50 years (Bloemendal et al., 2014). Among different seasonal underground thermal energy storage concepts, which stores energy underground, ATES is characterized by the highest storage capacities and is therefore most suitable for large-scale applications (Fleuchaus et al., 2018). In this type of systems, geological conditions play an important role in system performance. Among all the implemented projects, the Netherlands and Sweden are the market leaders and the number of ATES systems is expected to increase further (Fleuchaus et al., 2018).

2.2.1. Principles of ATES

According to the number of injection wells, ATES can be categorized as mono-well systems, doublet systems or multi-doublet (multiple pairs of doublet) systems (Fleuchaus et al., 2018). ATES mono-well contains one injection well, storing heat and cold thermal energy at different depth of the same location, while doublet systems contains two wells storing heat and cold energy at different location of a same aquifer (see Figure 2.2). The basic principle of a doublet ATES system operating over year is illustrated in Figure 2.3. In summer, ATES is operated to exchange for hot energy and store it in the hot well. Groundwater is extracted from the cold well and used for exchange the residual heat from the district heating network. The (relatively) cold energy is depleted through a heat exchanger. The heated up groundwater will be injected to the hot well and store for winter period. The exchanged cold energy can be used to ease the summer cooling demand. Heat pumps are optional to be added to the integration, in order to achieve the temperature required by the district heating and cooling system. To ensure a sustainable operation, all the water extracted from the cold store is re-injected into the warm store with no consumptive use of groundwater (Schmidt et al., 2018). In winter the process is reversed: water is pumped from the hot well and applied as a supplement heat source. After the heat transfer, the chilled water from the heat pump is injected into the cold well, recharging the cold energy storage for use in the following summer.

2.2.2. High Temperature Aquifer Thermal Energy Storage (HT-ATES)

According to the storage temperature of water, ATES can be classified as Low Temperature Aquifer Thermal Energy Storage (LT-ATES), which typically reaches up to 30 °C, and High Temperature Aquifer Thermal Energy Storage (HT-ATES) (Drijver et al., 2012). In the Netherlands, storage temperature between 30 - 60 °C is defined as medium temperature storage (MT-ATES), and systems with storage temperature higher than 60 °C are defined as HT-ATES (Drijver et al., 2012). This feature of HT-ATES enables the utilization of higher temperature heat sources (e.g. geothermal heat and wasted heat from combined heat and power plants), as evidenced by reference (Wesselink et al., 2018). In turns, high temperature storage has large potential to serve as direct heat source, and the required flow rate and

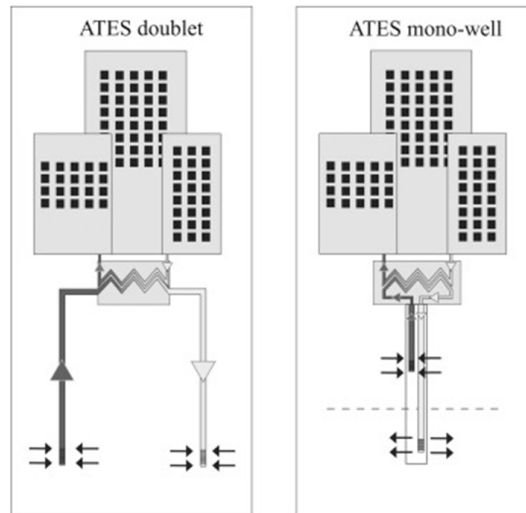


Figure 2.2: Illustration of mono-well system and doublet system of ATEs, adopted from (Fleuchaus et al., 2018)

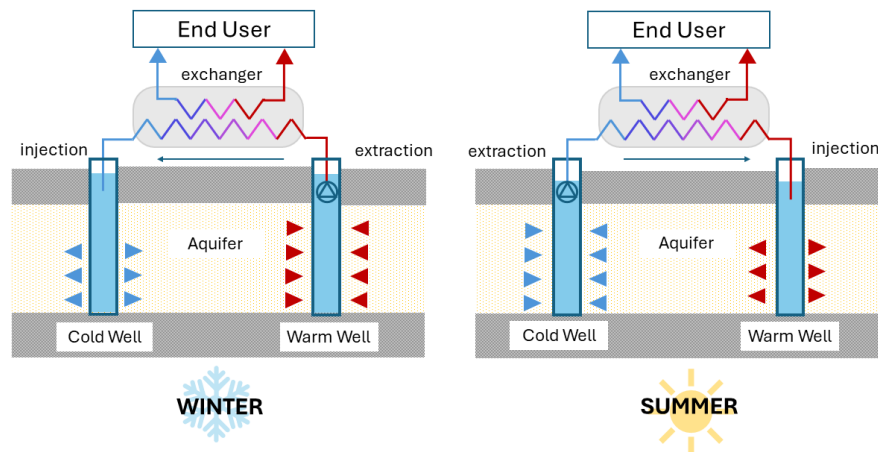


Figure 2.3: Operational scheme of ATEs system. Left: discharging hot energy during winter; Right: injecting the exchanged hot energy during summer

storage volume to supply the heat demand is lower than for regular ATEs (Drijver et al., 2012).

Currently, a limited number of HT-ATEs projects are operating worldwide. The main explanation of the constrained implementation is the more complex nature lies in the HT-ATEs. Despite the advantages of high temperature storage, the physical features of the utilized groundwater are largely impacted. This results in higher heat losses during active and storage phase, which in turns influence the thermal efficiency of the systems (see Chapter 3.1). Therefore, the modeling of the HT-ATEs systems is limited to represent the real-life situation due to the huge uncertainty of the heat losses underground. The complicated nature features can also result into unsatisfied thermal performance of the system and forced the project to be shut down (Dickinson et al., 2009). Additionally, the interactions between high temperature groundwater and the ambient environment can trigger geo-chemical reactions. To date, water treatments can be applied to prevent negative geo-chemical impacts such as precipitation of minerals and corrosion (Fleuchaus, Schüppler, Bloemendal, et al., 2020), while the effects on physical groundwater features are still significant to consider in design (Gao et al., 2017).

Furthermore, high store temperature results in higher heat losses during storage period and a long-term increase in subsurface temperature (Wesselink et al., 2018). As ATEs is typically installed in high density area where the subsurface fabric is complicated and sensitive to heat interference (Blo-

mendal et al., 2014), the aquifer selection of HT-ATES is strictly regulated. Application of HT-ATES in the shallow subsurface (< 500 m) is now not allowed in most European countries and also countries outside Europe because of legislation (Hähnlein et al., 2013). Therefore, the current HT-ATES in the Netherlands are all pilot projects.

2.3. Integration of ATES

In order to have a better understanding of the potential for optimization, the system integration of ATES is introduced in this section. This section starts with an introduction of the district heating and cooling system, followed by the integration of ATES in this system, including the illustration of the associated ATES schematic and operation.

2.3.1. District Heating and Cooling System

District heating (DH) connects buildings of various scales, from neighborhoods to entire country, through a network of pipes to provide space heating and domestic hot water. District cooling (DC) provides space cooling and process cooling to commercial and public building. There has been an increasing implementation of DC in industrial and residential sectors in recent years (L. Xu, 2020). Both DH and DC are now have reached the fourth generation (4GDH/C). This generation of the DH/C systems affords flexibility in the selection of energy sources, including conventional fossil fuels, waste heat and renewable energy sources. In the Netherlands, natural gas serves as the primary heat source for the majority of residences due to the substantial natural gas reserves in Groningen. In the light of transition to more climate-friendly future, the Dutch government anticipates that up to 50% of future heating systems in the built environment will be connected with District Heating networks by 2050 (Rojer et al., 2024). It can thus be seen that the integration of ATES into DH/C may be regarded as a potential solution which would contribute to achieving the climate goals.

2.3.2. System Integration

According to Schmidt et al. (2018), in Europe, around 100 of the 3000 existing ATES projects are large-scale systems integrated into district heating and cooling networks. ATES can be seen as a promising solution due to its long-term storage capability, which can overcome the seasonal mismatch between the availability of thermal energy and demand for heating and cooling. By implementing ATES, previously unused wasted heat in both heating and cooling sectors can be stored and used as an sustainable energy source. Furthermore, clean energy, including geothermal energy and solar energy, can also be stored. Figure 2.4 depicts a conceptual design of an HT-ATES integrated with a DHC network, illustrating the interconnections in operation during the winter mode. The groundwater is pumped out of the hot well and conveyed to the heat exchanger (HEX), where the heat is extracted from the groundwater and utilized to heat the water in supply lines. A heat pump can be optionally installed after the exchanger to raise the temperature to the desired level.

The returned cold energy is stored in groundwater from the same aquifer and injected to the cold well. The final recovered heat from the hot well is then added to the supply lines. In this configuration, the hot well discharge temperature is a result of the summer operation. In summer mode, the cold energy goes through a similar process and eventually added to the cold lines.

2.4. Optimization for ATES and Challenges

Currently, the optimization of the ATES systems are mainly focused on the individual performance (Fleuchaus, Schüppler, Godschalk, et al., 2020). In this type of study, the design parameters contributing to the thermal recovery efficiency are optimized to reduce heat loss and maximize the recovery rate. Stimulation models are widely applied for analysis the influential parameters under different scenarios (Bloemendal and Hartog, 2018; Behi et al., 2014; Fleuchaus, Schüppler, Godschalk, et al., 2020). The results emphasis the large impacts associated with the storage volume and geometry. Additionally, Sommer et al. (2015) studied the optimization of well placement to achieve highest investment reduction and the corresponding thermal recovery and environmental performance. This type of study also contributes to optimize the available subsurface space when designing ATES systems (Bloemendal et al., 2014).

Another type of optimization is to optimize the integration into DH/C. Cost optimization has been

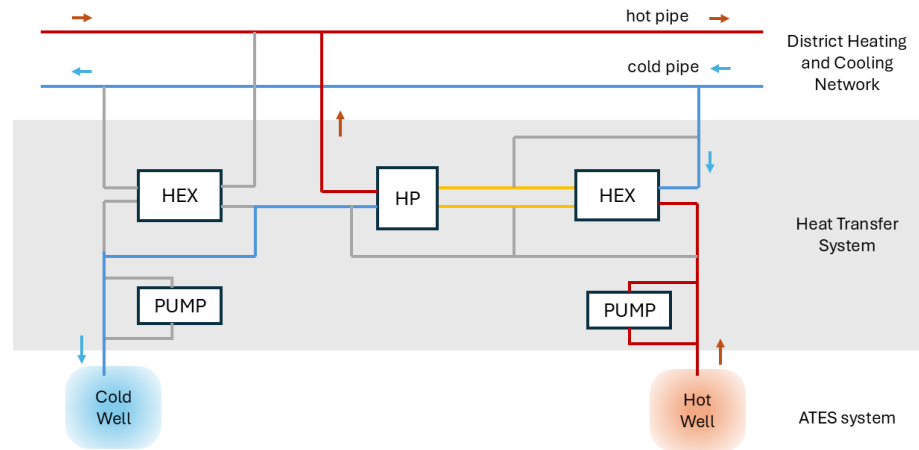


Figure 2.4: Schematic of ATEs integration into District Heating and Cooling Network, modified from (Remmelts et al., 2021). The system is operating in winter mode. In red the hot water streams, in blue the cold water streams and in grey the inactive lines for summer mode.

performed in designing for district heating or cooling system with thermal energy storage components (Khair and Haouari, 2015, Lozano et al., 2010). In this type of studies, MILP models are commonly formulated, where the thermal energy storage components are recognized as extra sources add to the system. Therefore, the aim of the system optimization are to optimize the capacity of the storage component, without diving into details of heat losses and the production efficiency.

As an complex system, the optimization of ATEs and the integration into DH/C have several difficulties. When optimizing the individual performance of the ATEs, various influential factors are essential to be taken into consideration. The thermal performance of ATEs is largely affected by the storage conditions and geometry (for details, see Chapter 3.1). The heat loss processes are determined by various factors ranging from geological conditions to operational parameters. Increasing the number of design parameters results in longer runtime and may needs external models (i.e groundwater model), while simplified model is limited to represent the real-life situation. Therefore, it is challenging to determine proper parameters to be include in the model.

For a systematic point of view, the optimization of ATEs integration is largely affected by the fluctuations in the DHC. To maintain an ATEs system, the thermal energy stored in the aquifer must be of a comparable magnitude to the extracted amount, in order to prevent short- or long-term temperature fluctuations (Pellegrini et al., 2019). This implies that, ideally, the heating and cooling demand from the building associated with the ATEs system should be equal. Study finds that in reality, most HT-ATEs systems were shut down due to an overestimated heating demand. An overestimated heating demand can result in surplus heat stored in hot wells after winter operation, which in turns leads to insufficient cold energy for summer cooling (Fleuchaus, Schüppler, Bloemendal, et al., 2020). Furthermore, alterations to the recovered temperature from the ATEs will also occur as a result of changes to the district heating network system.

3

Theoretical background

3.1. Heat transfer between network and the subsurface

The integration of the ATES systems is discussed in detail in Chapter 2, which addresses the cooperation of the subsurface systems and the DHC. This section presents a detailed analysis of heat transport in the subsurface, with a particular focus on the wells of the ATES system.

In ATES systems, injection typically occurs in a confined aquifer (Oerlemans, 2018). The permeability of the confining layer is low, which limits groundwater penetration in the vertical direction. Consequently, vertical flow through the top and bottom of the aquifer is negligible. The water is injected into the aquifer via the well screen, which has a maximum length equal to the thickness of the aquifer. Injection wells with a maximum well screen are considered to be fully penetrating wells. In the context of a fully penetrating well, the initial shape of the injected water can be regarded as that of a storage cylinder. The dimension of the cylinder depends on the injected volume (V_{in}), aquifer thickness (H) and porosity (θ). The hydraulic radius R_H of the cylinder can be calculated as:

$$R_H = \sqrt{\frac{V_{in}}{\theta H \pi}} \quad (3.1)$$

Due to thermal retardation, part of the heat is absorbed by the solid aquifer material. As a result, the thermal radius (R_{th}) is smaller than the hydraulic radius (R_H) with the influence of retardation factor (R_T):

$$R_{th} = \sqrt{\frac{V_{in}}{\theta H \pi R_T}} \quad (3.2)$$

Figure 3.1 visualizes the top and side views of the water and heat storage volumes.

During different operation phases, the storage geometry of the ATES increases when charging and decreases while discharging. As heat losses occur primarily at the outer surface where heated groundwater encounters ambient groundwater, the lowest heat loss can be achieved by identifying the lowest ratio of area to volume:

$$\frac{A}{V_{in}} = \frac{2}{L} + \frac{2}{R_{th}} \quad (3.3)$$

where L represents the length of the well screen associated with the inject/abstraction well. This value is equal to the thickness of the aquifer in the context of a fully penetrating well.

According to Doughty et al. (1982), the main processes causing heat loss in subsurface transport are: conduction, dispersion, groundwater flow, and density driven flow. Figure 3.2 illustrates the heat transfer processes in subsurface, including the effects of three different process specified in the sub-graphs (A to C). As shown in Figure 3.2A, dispersion occurs due to the variation of pore flow at the micro (grain) level. Mechanical dispersion plays a more significant role than molecular diffusion with respect to the flow induced by pumping.

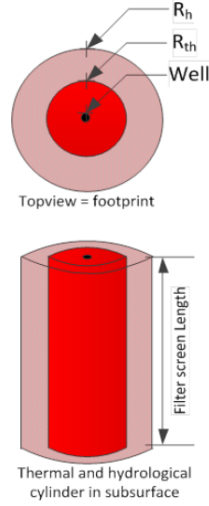


Figure 3.1: Hydraulic and thermal cylinder (Oerlemans, 2018)

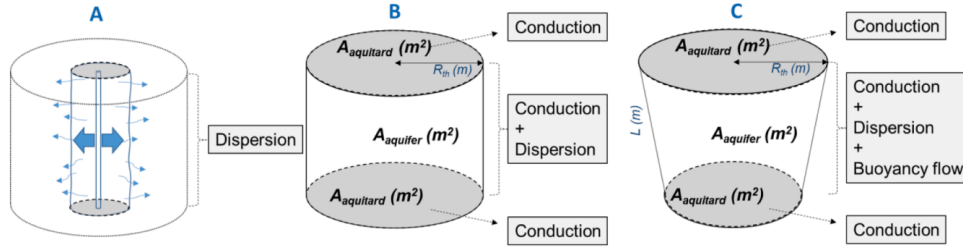


Figure 3.2: Heat loss process in subsurface (Beernink et al., 2024). In this graph: graph A illustrate the heat loss process generated by dispersion; graph B shows the combined effects of conduction and dispersion; graph C shows the impact of Buoyancy flow added to graph B

Given that vertical flow is negligible, the vertical dispersion into the aquitards is zero. The flow rate is observed to be at its highest near to the wellbore. Therefore, the greatest dispersion occurs in the area of the well and diminishes as the thermal front moves away from the well.

Conduction (see Figure 3.2B) occurs as a result of the temperature gradient between the boundary of the stored thermal volume and the ambient groundwater. The rate of conduction is dependent upon the thermal conductivity of the material, and is governed by Fourier's law. The losses due to conduction are found to decrease in proportion to the reduction in the ratio of A/V . For a given storage volume, the ratio of the A/V is smallest when L/R_{th} is equal to 2, indicating that the diameter of the thermal storage volume is equal to its height (Bloemendal and Hartog, 2018). While studies have suggested that for LT-ATES, conduction and dispersion mainly contribute to the heat loss due to lower temperature difference with ambient groundwater (Bloemendal and Hartog, 2018, Doughty et al., 1982), density driven flow plays an significant role in heat loss regarding high temperature storage.

Density driven flow, also referred to as buoyancy flow or free convection, is initiated by a density differential between the injected water and the ambient groundwater. It is one of the main contributor to the heat losses (Drijver et al., 2012). The higher density of the cold ambient water causes it to sink and accumulate at the base of the aquifer, while the lower density of the injected hot water causes it to rise and spread over the aquifer's cap. This creates a tilting thermal front which is illustrated in Figure 3.2C. The tilting phenomenon can contribute to significant heat losses and impact the thermal recovery efficiency (TRE). The TRE can be described as (Sommer et al., 2013):

$$n_E = \frac{\int_{extraction} Q_{ex}(T_{ex} - T_{amb})dt}{\int_{injection} Q_{inj}(T_{inj} - T_{amb})dt} \quad (3.4)$$

In the above equation, Q_{inj} and Q_{ex} are the corresponding water flow rate [m^3/s] during the entire

injection and extraction periods. T_{amb} is the ambient groundwater temperature [°C] and $T_{inj/ex}$ is the injected/extracted water temperature [°C]. The thermal recovery efficiency suggests the proportion of heat energy that can be recovered (or utilized) from the ATEs system in comparison to the heat energy injected. During winter operation, the density-driven flow phenomenon results in the retention of a portion of the injected hot water at the top of the aquifer. This leads to a reduction in the extracted heat and a corresponding decline in the TRE. Furthermore, the conical configuration of storage volume in turn influences the conduction losses, given that the surface area at the upper end of the thermal zone is greater than that at the bottom. This results in an increase in the A/V ratio.

3.2. Design and operational parameters

The design parameters of ATEs are related to multiple aspects. Figure 3.3 provides a summary of the major parameters considered during the design process, which are classified into three categories: subsurface characteristics, operational design, and system design.

Subsurface characteristics refer to aquifer selection, which have a significant impact on the heat loss process in the subsurface, as well as on the investment required for the project.

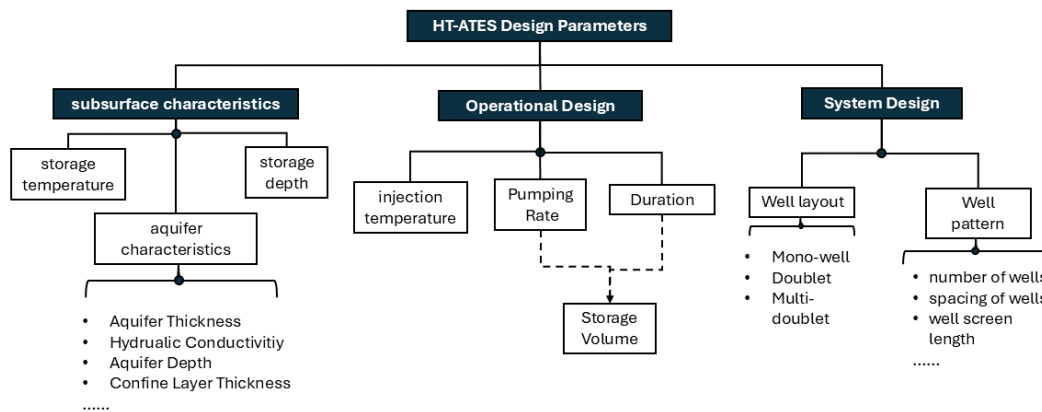


Figure 3.3: Summary of design parameters of ATEs

One of the parameters to consider is storage depth. As vertical thermal conduction can heat up the top and bottom aquitards (confining layers). Consequently, the selection of a deeper aquifer for HT-ATES results in a reduced degree of interaction with the shallow subsurface infrastructure. However, the use of a deeper aquifer requires greater pumping pressure, as well as an increased investment in drilling and pumping. In the Netherlands, the typical storage depth of ATEs systems ranges from -50 to -250 m, with an ambient groundwater temperature of 10 to 12 °C (Beernink et al., 2019). The design storage temperature there is to distinguish from injection temperature and it is applied to calculate the heat that is recovered from the ATEs and can be used for district heating. As illustrated by equation 3.4, thermal recovery efficiency is associated with the extraction temperature after storage period. Assuming there is no heat loss during extraction, the extracted thermal energy is equivalent to the stored energy. Therefore, the storage temperature can be regarded as the T_{ex} during the design phase. Accordingly, the discrepancy between the storage temperature and the ambient water temperature has a significant influence on the design of the efficiency of an individual ATEs system.

In reality, the storage temperature in the ATEs system varies due to different heat loss processes. As one of the most pivotal decisions to be made during the design phase, the characteristics of the aquifer have a significant influence on the loss of heat during the transfer and storage processes. For instance, an appropriate aquifer thickness permits the maximum vertical transfer height and influences the A/V . Aquifer with a thickness less than 10 m may leads to higher heat losses (Dinkelman and van Bergen, 2022). A increase in hydraulic conductivities can result in a higher titling rate. The Confine layer thickness also has an impact on vertical heat conduction. In case of 90 °C of heat, a confining layer of 30 m thickness with a resistance of at least several thousand days is sufficient for 20 years of operation (Drijver et al., 2012).

In addition to the selection of the aquifer, the operational design parameters emphasize the parameters that can be adjusted during operation. The initial step in the design process is to determine the optimal range of injection temperatures for the ATES. The pumping rate and duration are frequently combined to determine the storage volume, which is defined as the total volume of water stored in the wells. An increase in storage volume will result in an improvement in thermal recovery efficiency (Beernink et al., 2024).

System design parameters includes well layout and well patterns, which are significant to consider in the integration in district heating, especially in the context of large-scale ATES systems comprising multiple wells.

It is also important to have a systematic view of all these design parameters and understand the interaction between them. For instance, the buoyancy flow created by high injection temperature of water can be mitigated by selecting an aquifer with lower permeability and a higher ambient temperature (Drijver et al., 2012; Drijver et al., 2019). The impact of high conductivities can be reduced by the implementation of multiple partially penetrating wells instead of wells with a single long well screen (Dinkelman and van Bergen, 2022).

3.3. Differences with daily storage buffer tanks

Buffer tanks, or thermal storage tanks, are insulated individual units designed to store heat. The system illustration of tank thermal storage and aquifer thermal energy storage is presented in Figure 3.4.

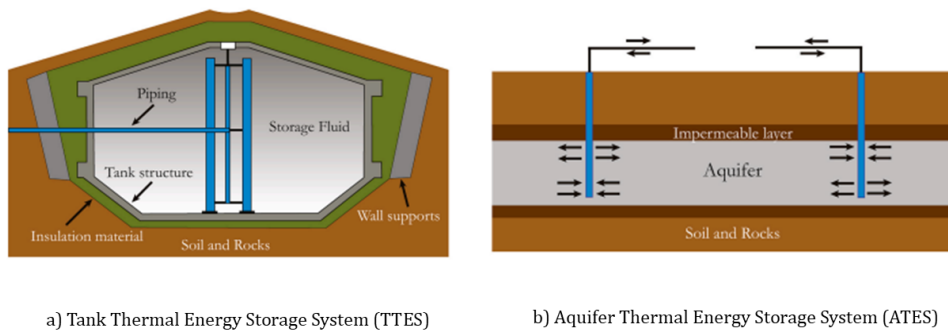
One of the main difference between ATES systems and buffer tanks is the storage capacity. Buffer tanks store hot water within a constructed fixed volume and the thermal mixing occurs within the tank with ambient air temperature (Sarbu and Sebarchievici, 2018). The available storage capacity of these tanks is determined by a filling degree factor and the tank's maximum volume. In ATES systems, the extracted thermal energy is transferred to the heating network via a heat exchanger, whereas buffer tanks supply stored hot water directly to the network, eliminating the need for a heat exchanger.

Heat loss mechanisms differ significantly between ATES systems and buffer tanks. ATES systems experience more interactions with the surrounding environment that can lead to heat loss. For instance, the stored heat in the system is largely impacted by the groundwater flow and ambient temperature, while the buffer tank is limited affected by external condition as being insulated and isolated. Heat losses also occur at the exchanger for ATES systems, while for the buffer the heat exchanger is not required.

Consequently, the storage capacity of buffer tanks are confined by their physical volumes. Hot water storage systems used as buffer storage for DHN supply are usually in the range of 500 L to several m³ (Sarbu and Sebarchievici, 2018).

In the contrast, ATES systems are more suitable for large scale energy storage with no exchange with the water in heating network. In ATES systems, "cold" return energy is captured through the heat exchanger with designed efficiency and stored in the cold well of the system. While it is not feasible to stored the the "cold" energy in the same buffer tank and the return temperature is determined by the heating system's demand. For a controllable cooling purpose, the integrated system requires additional application of the tanks at the cooling plant.

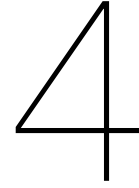
In accordance with the system capacity, buffer tanks are commonly applied for daily thermal storage, whereas ATES systems are more suitable for seasonal storage. Daily storage systems integrated in DH systems are mainly designed to tackle the significant load fluctuations throughout the day. The necessity for heat and cold can vary according to the specific end-use, individual habits, type of heating device, regulatory equipment etc (Guelpa & Verda, 2019). Consequently, integrated buffer tanks are capable of operating in a flexible manner in order to compensate for the daily peak demand. The heat losses of a buffer are approximately 5% of the injected energy (Guelpa & Verda, 2019). ATES systems are most commonly integrated for long-term storage. ATES systems are capable of storing injected energy for several months, allowing stored energy utilization in other seasons. The typical operational scheme of an ATES system comprises 4 phases: charge, storage, rest and discharge. In comparison to buffer tanks, ATES systems have a longer storage period and additional rest period, resulting in a higher heat loss. Consequently, the total heat loss of ATES systems can reach up to 30% of the injected energy (J. Xu et al., 2014).



a) Tank Thermal Energy Storage System (TTES)

b) Aquifer Thermal Energy Storage System (ATES)

Figure 3.4: System illustration of different technology: a) Tank thermal energy storage and b) Aquifer thermal energy storage



Methodology

4.1. Optimization method

The optimization software used in this study is **rtc-tools** developed by Deltares with an extension package, **rtc-tools-heat-network**, developed within [WarmingUP project](#) in collaboration with TNO. It is built based on the **rtc-tools**, which is an optimization application for optimal planning, design and operation of Energy Systems with the current main focus on District Heating Systems (DHS). The project version applied in this study is 0.1.8, which implemented **Modelica** language as the main method for defining the energy system. Modelica language is a kind of open language which allows development and specification of corresponding modeling libraries used for system modelling and stimulation. As engaged in the WarmingUP Project, a project focusing on sustainable heat transition, a library of modeling the heat network components was developed and interact with the **rtc-tools-heat-network**.

The optimization package hosts two optimization approaches: 1) Mixed Integer Linear Problem (MILP) approach and 2) Nonlinear Problem (NLP) approach to solve different part of the formulated problem. The comparison between the two approaches are listed as below:

1. The (MI)LP has as decision variables: the discharge, the head, and most notably the heat flow rate. By using the heat flow rate as a variable instead of the temperature, we can get rid of the non-linear mixing constraints.
2. The NLP that has as decision variables: the discharge, the head, and most notably the temperature. The NLP has fixed flow directions (following from the MILP).

4.2. Software: rtc-tools

4.2.1. library construction

As the numerical models are developed in external software, such as Modelica and ESDL, the primary role of `rtc-tools-heat-network 0.1.8` is to interpret and optimize the energy systems. The software library contains three main sub-folders: `esdl`, `modelica` and `pycml`, storing different types of files, respectively. In this study the focus is the cooperation of modelica files and Python files. Modelica files with a suffix `.mo` are built to defined the components with essential parameters specified as inputs and outputs. The alterable parameters are also noted in the modelica model. According to the type of optimization problem mentioned above, the corresponding modelica components (`.mo`) are developed for MILP and NLP problem respectively. `Pycml` (Python component library) folder stores Python files that are built to parse modelica variables into python language as CasDAi components, which is an symbolic system helps with optimization discretization. Therefore the `pycml` library contains individual `.py` files sharing the same name and definitions with the modelica model components. Figure 4.1 illustrated the construction of the `rtc-tools-heat-network` library, highlighting significant components related to this study.

As shown in the Figure 4.1, the `Heat` folders contains modelica componets(`.mo`) constructed for `HeatProblem` (MILP) while `QTH` folder is designed for `QTHProblem` (NLP).The corresponding heat network components(`.py`) are stored in the `pycml>component_library.pycml>model_base.py`

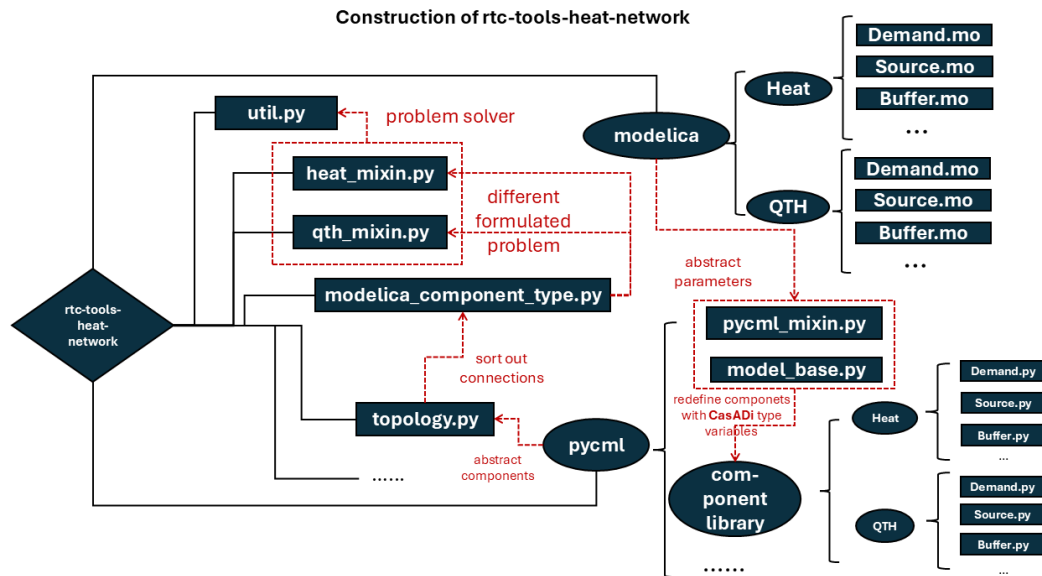


Figure 4.1: Construction of rtc-tools-heat-network: individual files are shown in rectangular shape while folders are shown in oval shape.

and `pycml>pycml_mixin.py` are established to convert variables of the components (.py) suitable for CasADi symbolic systems. The developed components (.py) are added to `topology.py` and the internal connections and flow directions are sorted out in `modelica_component_type.py`. The iterations and computation is done through the `HeatMixin.py` and `QTHMixin.py`, according to the formulated problem. An example workflow of solving heat problem with `rtc-tools-heat-network` is present in Figure 4.2.

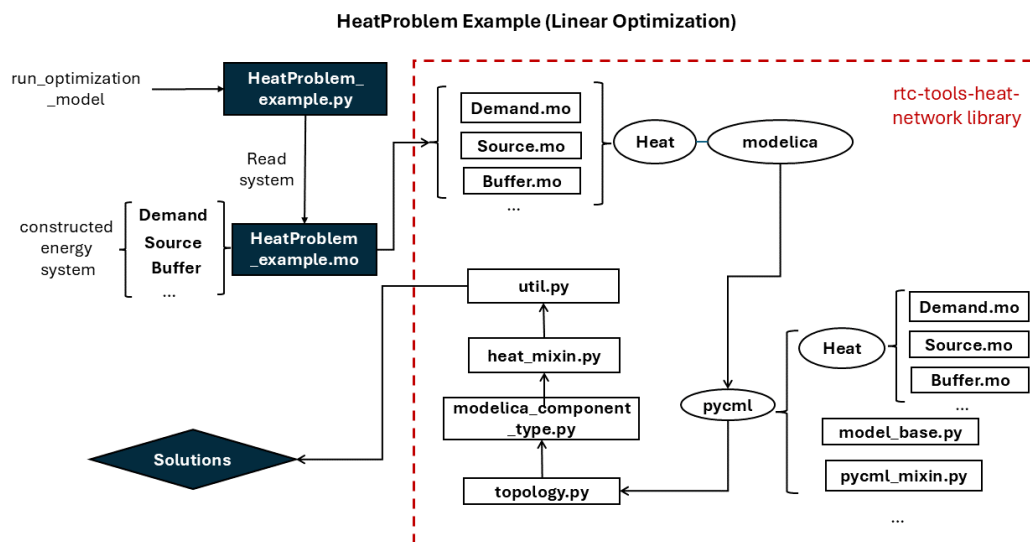


Figure 4.2: Example workflow of solving heat problem

4.2.2. Heat Problem

In this section, the concept of *HeatProblem* is explained, including the construction of components and heat flow rate.

Components

First of all, components constructed in response to the heat problem are specified as a type of `HeatPort`. The designation of `HeatPort` indicates that the components have several attributes that relate to heat storage or transfer. The variables associated with a `HeatPort` are as follows: `Heat` (Heat flow rate [W]), `Q` (flow rate [m³/s]) and `H` (Head [m]). Building on this, a component that has both thermal inflow and outflow is defined as a type of `HeatTwoPort`. Such components comprise an `Inport` and an `Outport`, whereby the heat flow rate flows in and out of the component. The corresponding variables added are `Heat_In` and `Heat_Out`. The components mentioned in the following are all falls under the category of `HeatTwoPort` components.

Furthermore, a component that does not serve the function of thermal energy storage can be classified as an `_Non_storage_component`, where the gains (fluxes to the `Inport`) and releases (fluxes leaves the `Outport`) are the same. Both the `Source` and the `Demand` are developed as non-storage component. The `Source` component is developed to represent the heat sources (i.e., combined heat and power plants) in real-life scenarios. A minimum and maximum mass of heat is defined as the capacity of the source. Similarly, the `Demand` component is developed to represent the behavior of the end users, which is represented by an input of a time series of heat. The heat delivered through the supply pipelines is connected to the `Inport`. Once the demanded energy has been deducted, the residual heat leaves the `Outport` and is applied to the return lines. The return lines are linked back to the sources. Subsequently, the heat from the return lines is conveyed into the `Inport` of the sources. `Buffer` is constructed as a storage component distinguish from non-storage components. It is explained in detail in Section 4.2.3

Heat flow rate formulation

As aforementioned, the heat flow rate (P [J/s]), is one of the significant decision variables formulated in heat problem and the numerical equation is illustrated as follow:

$$P = \rho c_p Q T \quad (4.1)$$

In the equation, ρ is the density of water [kg/m³], c_p is the heat capacity [J*kg⁻¹*°C⁻¹], Q is the flow rate [m³/s] and T is temperature [°C]. The units of different parameters can be specified in the Modelica models in accordance with the `Modelica.SIunits` library. During the investigation of the `rtc-tools-heat-network` library, it was observed that in some components, the distinction between heat flow rate [J/s] and heat [J] is not explicitly made. However, this has a limited impact on the optimization process. Based on the library's construction, as outlined in section 4.2.1, all components developed in Modelica are translated into Python, with only the parameters abstracted. The physical quantities of these parameters are defined through equations. Consequently, the units originally defined in the Modelica models appear to be of less importance, and the Modelica library treats "Heat" as a general term, differentiating it primarily from "Volume".

The temperatures in the system typically range from 10 to 100 °C, which can lead to very large offset when modelling. In addition, various temperatures in different locations also need to be specified when applying the above equations. To mitigate the impacts, a relative formulation is used, where the heat flow rate is set to be zero at some point in the system, typically at the return lines, i.e upstream of all sources and downstream of all demands. This relative formulation uses dT which is a fixed temperature difference to formulate the linear optimization problem and the values are calculated at the demands. Therefore, the equations can be illustrated as the following:

$$dT = T_{demand,in} - T_{demand,out} \quad (4.2)$$

$$P_{demand,in} = \rho c_p Q_{demand,in} dT \quad (4.3)$$

$$P_{demand,out} = 0 \quad (4.4)$$

In the above equations, subscript *in* and *out* is used to differentiate the `Inport` and `Outport` of the component. The return lines are connected to the in port of all sources where all heat flow rate are

defined as zero. With heat losses in the system, the sources need to produce strictly more heat than is consumed by the demands. Therefore the sources have the following relationships:

$$P_{source,in} = 0 \quad (4.5)$$

$$P_{source,out} \geq \rho c_p Q_{source,out} dT \quad (4.6)$$

Without specifying anything for the pipes, this could still lead to infeasible solutions. For example, an infeasible solution may be that the heat flow rate through a pipe with zero flow is much larger than its heat loss. Therefore an optimal solution would be found where the heat flow rate to one of these pipes is exactly equal to its heat loss. `Pipe` is also developed as a `HeatTwoPort` type of component in the library. Assuming positive flow:

$$P_{pipe,in} \geq \rho c_p Q_{pipe,in} dT \quad (4.7)$$

$$P_{pipe,out} \geq \rho c_p Q_{pipe,out} dT \quad (4.8)$$

4.2.3. Storage component: Buffer

As formulated in *HeatProblem*, the heat flow rate (P [J/s]) added or extracted from the buffer is attribute to variable `Heat_buffer`. The heat (E [J]) stored in the buffer is attribute to variable `Stored_heat`. `Heat_loss` in buffer is modeled as linear with the stored heat: assuming heat loss happening in every time step of storing with a loss coefficient. The following relationships can be defined:

$$\frac{\partial E_{stored}}{\partial t} = P_{buffer} - P_{loss} \quad (4.9)$$

$$P_{loss} = E_{stored} \beta_{loss} \quad (4.10)$$

Where β_{loss} is heat loss coefficient. The loss coefficient is approximated assuming that tanks are cylindrical and lose heat over the surface area. The heat loss function of cylinder (with a radius equals R [m]) is applied to calculate the coefficient:

$$\beta_{loss} = 2 * \beta_{transfer} / (R * \rho * c_p) \quad (4.11)$$

Where $\beta_{transfer}$ is the heat transfer coefficient of related material, in this case water. The typical value of water is 1 (W/(m²·K)) and applies in the equation.

As aforementioned in Section 3.3, the buffer can be recognized as a cylinder with height and radius predefined, the storage of heat has upper and lower boundaries determined by a minimum filling rate α_{min} (default=0.05) and a maximum confined by the volume, computed as the following:

$$E_{min} = V \alpha_{min} dT c_p \rho \quad (4.12)$$

$$E_{max} = V(1 - \alpha_{min}) dT c_p \rho \quad (4.13)$$

5

Buffer Model Setup

5.1. Heating Network

The initial model is built to gain a better understanding of the system and implementing the problem solver. The initial model is comprised of a Modelica model and a time series of heat demand from 2013-5-19 22:00 to 2013-5-21 18:00 with a time step of 1 hour. The schematic is illustrated as Figure 5.1.

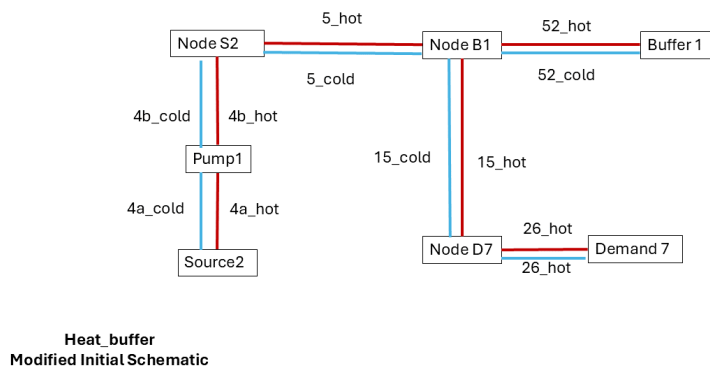


Figure 5.1: Schematic of the initial model: The red lines indicate the supply lines and the blue lines are return lines, pipes are connected at the nodes

The problem is developed as a `HeatProblem`, therefore the heat transferred in the system is designed as heat flow rate (see Chapter 4.2.2). The primary heat supplier in this system is `Source 2`, which has a delivery capacity of 0 to 1,500,000 J/s in terms of heat flow rate. A pump (`Pump 2`) is added to pump the water from the source to the system. A buffer (`Buffer 1`) is added as a storage component. The buffer tank is defined as a cylinder with a radius (R) of 10 m and a height (H) of 5 m and the minimum filling rate (α_{min}) of the tank is 0.05. In this setup, the density (ρ) of water is 988 kg/m³ and the specific heat capacity (c_p) of water is 42000 J/(kg·°C). These parameters are applied in the equations specified in section 4.2.3 to calculate the heat stored in the buffer at every time step. The modeled system has only one end user (`Demand 7`), whose behaviors is provided by the input time series.

Components are connected with supply and return lines, illustrated as red and blue lines in the schematic (Figure 5.1) respectively. The temperature in all the supply and return lines are fixed, with a

supply temperature of 75 °C and a relatively cold return temperature of 45 °C. The heat being transferred in the system is calculated as the relative heat, which is the difference of heat flow rate between the supply lines and the return lines. According to equation 4.1, dT is the fixed temperature difference between the supply and return lines, ρ and c_p are constant, therefore the heat flow rate is linear to the flow rate of water carrying the heat.

5.2. Scenarios

In this model, thermal energy supply from the source is sufficient (maximum delivery rate = 1,500,000 J/s) and fluctuates with the requirement of the demand on an hourly basis. The heat demand is higher during daytime, hitting more than 250,000 J/s and stays at around 150,000 J/s during nighttime. Therefore a buffer is added to supply for the hourly peaks during the day and maintain a stable production from the source.

The goals are listed as the following:

1. Meet the demand,
2. Keep the production of source 2 constant.

The constraints are listed as the following:

1. Activate the buffer only when the demand is larger than source production.
2. Demand should be supplied by the demand and buffer (no external supplier).

6

Result Analysis

The results are present in Figure 6.1, which provides the fluctuations of demand, the source production and the buffer in terms of heat flow rate. The x axis is time [h], the y axis is heat [J/s].

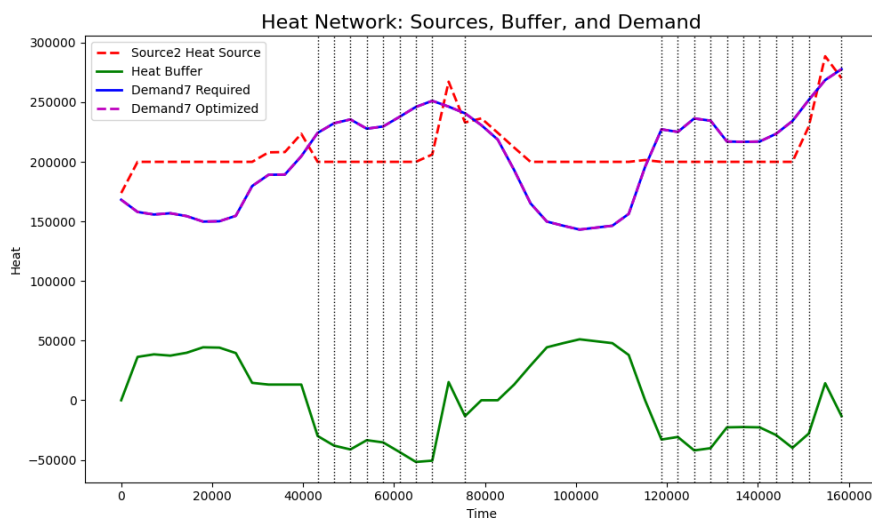


Figure 6.1: The heat of source, demand and buffer, dashed lines indicate the time when the demand is larger then the source is activated

The red dashed line is the production of the source, maintained at around 200,000 J/s, which is a middle value of the required demand mentioned in section 5.2. It is notable that the demand can always be met, resulting in the optimized demand and the real demand series being overlapped in the graph. The green line represents the fluctuation of the heat flow rate that goes in and out of the buffer. Positive values indicate an injection phase, while negative values represent an extraction phase. Therefore, two injection phases can be clearly observed from time step 0 to 4000 and from around 8000 to 120,000, as the heat flow rate values are positive. The vertical dashed lines indicate the time at which the demand exceeds the stable delivery of the source. For example, vertical lines are presented from time step 42,000 to 70,000, during which the demand (purple line) exceeds the source production (red dashed line). Meanwhile, the buffer is being activated and discharging. This behavior is consistent with the objective of compensating for the hourly peak demand through the application of a buffer. Nevertheless, the activation of the buffer is only depends on the heat deficit, which results in discontinuity in operation. For instance, the buffer starts injecting at around time step 73,600 for an hour and suddenly switch to discharge mode at the next hour.

7

Discussion

In this context, the buffer is optimized for the daily storage and delivery of energy. Consequently, the operation of the buffer is highly sensitive to the hourly discrepancy between the source and demand. The pumps are in active operation, facilitating the transfer of water to the exchanger, which requires greater energy and incurs greater pump degradation. The current composition of the buffer is primarily designed for operational optimization, with limited consideration given to design optimization. The capacity of the buffer is constrained by its volume, which must be altered manually. In this model, the source is sufficed to meet all the required demand without adding a buffer (see Figure 7.1), thereby allowing for significant potential for optimization. In the event that the source has limited capacity or a smaller buffer tank, the optimization is limited to provide a robust operation scheme.

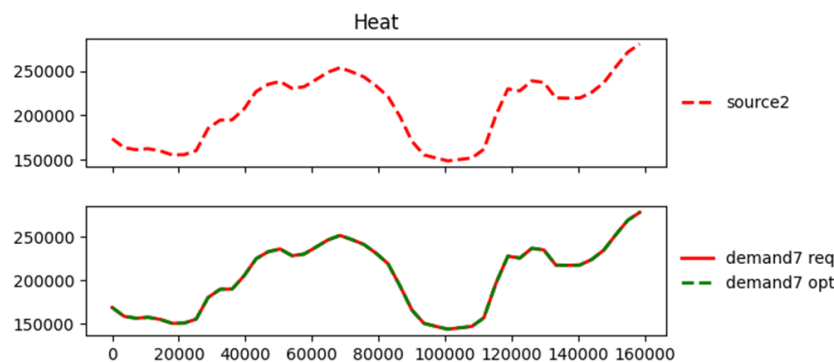
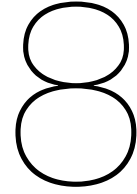


Figure 7.1: The same model without a buffer: x axis is time[h], y axis is heat flow rate [J/s], the behavior of source(upper plot), demand and the optimized demand (lower plot) are in accordance

The objective of this internship is to enhance the functionality of the daily storage component to encompass seasonal storage, which will be achieved by developing an ATEs component within the rtc-heat-network library. The study has encountered several challenges. Firstly, the composition of the rtc-tools-heat-networks is highly complex, which contains internal cooperation between Modelica models and Python components. The lack of comprehensive documentation on these internal links has resulted in a longer process than originally anticipated. Following an investigation into the software, a fundamental understanding of the process for developing a component within the library has been acquired. Nevertheless, it is challenging to add a component and validate the entire physical composition within a limited internship period. As previously stated, the heat loss processes in the ATEs are diverse. In the case of HT-ATEs, the dominated process is the buoyancy flow. This is a consequence of the interaction between hydraulic and heat transfer processes. The heat loss currently considered

in the buffer component is solely dependent on the geometry of the tank, without the influence of the complex underground heat loss process. The resulting heat losses coefficient is a proportional to the total volume of the buffer tank and applies to each time step. In order to be able to optimize the capacity of HT-ATES, it is necessary to redefine the corresponding heat losses. One of the simplified method to model the heat losses for ATES is to only consider the losses resulting from temperature fluctuations. In the OMOTIS project developed for optimization of energy system, the heat loss is calculated from the temperature difference per time step. The temperature loss varies within the range of minimum and maximum temperature change per time step, therefore the temperature difference is not fixed as in this study. As a result, heat loss per time step is calculated through the equation of heat flow rate (equation 4.1). This approach to problem formulation allows the storage component to be designed with a flexible geometry, thereby facilitating the optimization of storage capacity. Nevertheless, this type of modelling requires time series data regarding temperature variations within the district heating system. The OMOTIS project has been developed with the objective of cooperating with the modeling language ESDL (Energy System Description Language), which has not been applied in this study. In order to proceed with the existing modeling tools, this study attempted to calculate the heat losses associated with the injected and stored water volume. Similarly, the heat losses are calculated as a heat loss coefficient multiplied by the storage volume over a given time step. In contrast to the fixed cylinder shape of the tank, the ATES is constructed as a flexible cylinder that can expand or contract in accordance with the injected or extracted water volume. Nevertheless, the change of the volume and the radius has a non-linear relationship, resulting an unfeasible solution with linear solver.



Conclusions and recommendations

This study provides a concise overview of various thermal energy storage technologies and explains the heat transfer process between ATES and district heating and cooling networks. To develop an HT-ATES component for linear optimization, an investigation into the existing buffer component was conducted to enhance understanding. During this process, the interactions between Modelica models and Python components were documented. Based on the buffer, this study attempts to create a storage component with a flexible radius as a starting point. A linear solver is applied for a simple problem formulation, where heat losses were represented as a heat loss coefficient multiplied by the storage volume per time step. However, due to limitations in knowledge and time, the storage component was not fully developed. A potential schematic of a doublet ATES component integrated in a district heating network (DHN) is illustrated in Figure 8.1. In this formulation, the cold well and hot well are modeled separately. The temperature, water flow rate, and corresponding storage volume are separated to represent the behavior in different phases. Heat losses are mainly considered at the heat exchanger and during the storage phase of the hot well and the cold well.

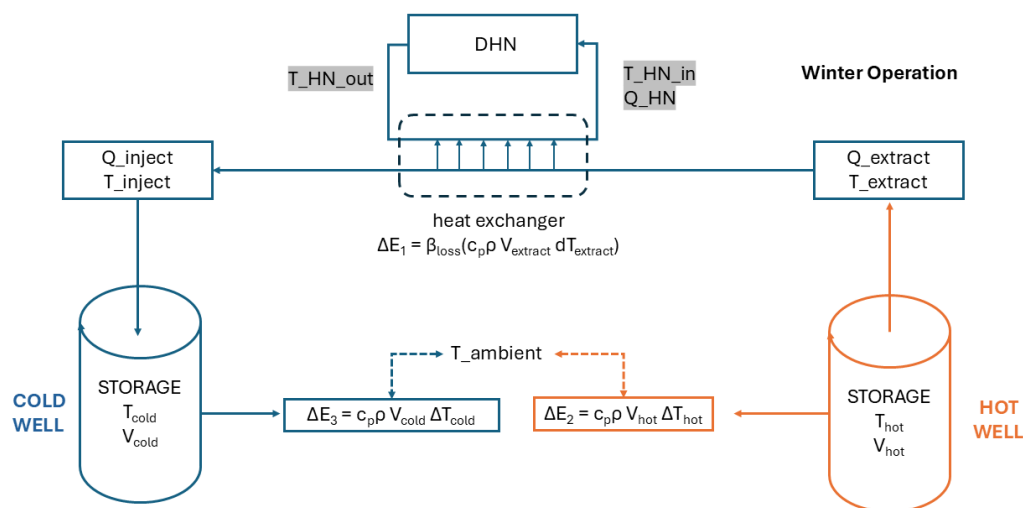


Figure 8.1: A potential schematic of ATES component integrated in DHN in winter operation: Cold wells and Hot wells are modeled separately, T is temperature, Q is water flow rate, V is storage volume. Heat losses (E) happen during storage phase (temperature loss (ΔT) with the influence of ambient temperature) and at the exchanger (proportional to the extracted heat, with a loss coefficient β_{loss})

It is important to notice that the groundwater used in the ATEs has no exchange with the water in the DHN lines, therefore the flow rate and temperature of the DHN and ATEs are different. Based on this formulation, two influential parameters regarding the design heat storage capacity of ATEs are storage volume (V) and temperature loss (ΔT). Firstly, the geometry of the cold and hot wells must be identified. In order to optimize the capacity of the system, it is recommended that a flexible radius formulation be used to model the storage volume at each time step. In some cases, a non-linear solver may be necessary to address this type of problem. The temperature loss that occurs during the storage phase can be attributed to a number of different heat loss processes, which are discussed in Chapter 3.1. Different design parameters (3.2) are found to have different impacts on these heat loss processes. It is therefore recommended that future studies can begin with the running of stimulation models in order to identify the relationship between the design parameter and the temperature loss, which can then be applied to represent temperature loss. Furthermore, the storage temperature is subject to influence from the ambient groundwater temperature, which can be added to the scenarios when the stimulation model is executed.

Bibliography

- Alva, G., Lin, Y., & Fang, G. (2018). An overview of thermal energy storage systems. *Energy*, *144*, 341–378.
- Beernink, S., Hartog, N., Bloemendal, M., & van der Meer, M. (2019). Ates systems performance in practice: Analysis of operational data from ates systems in the province of utrecht, the netherlands. *Proceedings of the European Geothermal Congress, 2019*, 11–14.
- Beernink, S., Hartog, N., Vardon, P. J., & Bloemendal, M. (2024). Heat losses in ates systems: The impact of processes, storage geometry and temperature. *Geothermics*, *117*, 102889.
- Behi, M., Mirmohammadi, S. A., Suma, A. B., & Palm, B. E. (2014). Optimized energy recovery in line with balancing of an ates. *ASME Power Conference, 46094*, V002T09A002.
- Bloemendal, M., & Hartog, N. (2018). Analysis of the impact of storage conditions on the thermal recovery efficiency of low-temperature ates systems. *Geothermics*, *71*, 306–319.
- Bloemendal, M., Olsthoorn, T., & Boons, F. (2014). How to achieve optimal and sustainable use of the subsurface for aquifer thermal energy storage. *Energy Policy*, *66*, 104–114.
- Dickinson, J., Buik, N., Matthews, M., & Snijders, A. (2009). Aquifer thermal energy storage: Theoretical and operational analysis. *Geotechnique*, *59*(3), 249–260.
- Dinkelman, D., & van Bergen, F. (2022). Evaluation of the country-wide potential for high-temperature aquifer thermal energy storage (ht-ates) in the netherlands. *European Geothermal Congress*, 9.
- Doughty, C., Hellström, G., Tsang, C. F., & Claesson, J. (1982). A dimensionless parameter approach to the thermal behavior of an aquifer thermal energy storage system. *Water Resources Research*, *18*(3), 571–587.
- Drijver, B., Bakema, G., & Oerlemans, P. (2019). State of the art of ht-ates in the netherlands. *European Geothermal Congress: Proceedings, Den Haag, Netherlands*.
- Drijver, B., van Aarssen, M., & Zwart, B. D. (2012). High-temperature aquifer thermal energy storage (ht-ates): Sustainable and multi-usable. *Proceedings of the Innostock*, 1–10.
- Fleuchaus, P., Godschalk, B., Stober, I., & Blum, P. (2018). Worldwide application of aquifer thermal energy storage—a review. *Renewable and Sustainable Energy Reviews*, *94*, 861–876.
- Fleuchaus, P., Schüppler, S., Bloemendal, M., Guglielmetti, L., Opel, O., & Blum, P. (2020). Risk analysis of high-temperature aquifer thermal energy storage (ht-ates). *Renewable and Sustainable Energy Reviews*, *133*, 110153.
- Fleuchaus, P., Schüppler, S., Godschalk, B., Bakema, G., & Blum, P. (2020). Performance analysis of aquifer thermal energy storage (ates). *Renewable Energy*, *146*, 1536–1548.
- Gao, L., Zhao, J., An, Q., Wang, J., & Liu, X. (2017). A review on system performance studies of aquifer thermal energy storage. *Energy Procedia*, *142*, 3537–3545.
- Gil, A., Medrano, M., Martorell, I., Lázaro, A., Dolado, P., Zalba, B., & Cabeza, L. F. (2010). State of the art on high temperature thermal energy storage for power generation. part 1—concepts, materials and modellization. *Renewable and sustainable energy reviews*, *14*(1), 31–55.
- Guelpa, E., & Verda, V. (2019). Thermal energy storage in district heating and cooling systems: A review. *Applied Energy*, *252*, 113474.
- Hähnlein, S., Bayer, P., Ferguson, G., & Blum, P. (2013). Sustainability and policy for the thermal use of shallow geothermal energy. *Energy Policy*, *59*, 914–925.
- Khair, R., & Haouari, M. (2015). Optimization models for a single-plant district cooling system. *European Journal of Operational Research*, *247*(2), 648–658.
- Lanahan, M., & Tabares-Velasco, P. C. (2017). Seasonal thermal-energy storage: A critical review on btes systems, modeling, and system design for higher system efficiency. *Energies*, *10*(6), 743.
- Lozano, M. A., Ramos, J. C., & Serra, L. M. (2010). Cost optimization of the design of chcp (combined heat, cooling and power) systems under legal constraints. *Energy*, *35*(2), 794–805.
- Oerlemans, P. J. (2018). *Modelling heat transport in a high temperature ates system* [Master's thesis, Utrecht University].

- Pellegrini, M., Bloemendal, M., Hoekstra, N., Spaak, G., Gallego, A. A., Comins, J. R., Grotenhuis, T., Picone, S., Murrell, A., & Steeman, H. (2019). Low carbon heating and cooling by combining various technologies with aquifer thermal energy storage. *Science of the Total Environment*, 665, 1–10.
- Pompei, L., Nardecchia, F., & Miliuzzi, A. (2023). Current, projected performance and costs of thermal energy storage. *Processes*, 11(3), 729.
- Remmelts, J., Tensen, S., & Ferreira, C. I. (2021). Seasonal thermal energy storage for large scale district heating. *13th IEA heat pump conference; 26.-29.04. 2021; jeju, korea. Borås, Sweden*, 1633–1643.
- Rojer, J., Janssen, F., van der Klauw, T., & van Rooyen, J. (2024). Integral techno-economic design & operational optimization for district heating networks with a mixed integer linear programming strategy. *Energy*, 308, 132710.
- Sadeghi, H., Jalali, R., & Singh, R. M. (2024). A review of borehole thermal energy storage and its integration into district heating systems. *Renewable and Sustainable Energy Reviews*, 192, 114236.
- Sarbu, I., & Sebarchievici, C. (2018). A comprehensive review of thermal energy storage. *Sustainability*, 10(1), 191.
- Schmidt, T., Pauschinger, T., Sørensen, P. A., Snijders, A., Djebbar, R., Boulter, R., & Thornton, J. (2018). Design aspects for large-scale pit and aquifer thermal energy storage for district heating and cooling. *Energy Procedia*, 149, 585–594.
- Solé, A., Martorell, I., & Cabeza, L. F. (2015). State of the art on gas–solid thermochemical energy storage systems and reactors for building applications. *Renewable and Sustainable Energy Reviews*, 47, 386–398.
- Sommer, W., Valstar, J., van Gaans, P., Grotenhuis, T., & Rijnaarts, H. (2013). The impact of aquifer heterogeneity on the performance of aquifer thermal energy storage. *Water Resources Research*, 49(12), 8128–8138.
- Sommer, W., Valstar, J., Leusbrock, I., Grotenhuis, T., & Rijnaarts, H. (2015). Optimization and spatial pattern of large-scale aquifer thermal energy storage. *Applied energy*, 137, 322–337.
- Wesselink, M., Liu, W., Koornneef, J., & van Den Broek, M. (2018). Conceptual market potential framework of high temperature aquifer thermal energy storage-a case study in the netherlands. *Energy*, 147, 477–489.
- W.P.Rocchi. (2020). Improving identification of ht-ates performance drivers and -barriers | tu delft repository. <https://resolver.tudelft.nl/uuid:af03ff94-c98f-48c1-967d-a92010774d28>
- Xu, J., Wang, R., & Li, Y. (2014). A review of available technologies for seasonal thermal energy storage. *Solar energy*, 103, 610–638.
- Xu, L. (2020). Design optimization of seasonal thermal energy storage integrated district heating and cooling system: A modeling and simulation approach.
- Zhang, H., Baeyens, J., Cáceres, G., Degreve, J., & Lv, Y. (2016). Thermal energy storage: Recent developments and practical aspects. *Progress in Energy and Combustion Science*, 53, 1–40.